minerals

MDPI

Article

Employing Statistical Algorithms and Clustering Techniques to Assess Lithological Facies for Identifying Optimal Reservoir Rocks: A Case Study of the Mansouri Oilfields, SW Iran

Seyedeh Hajar Eftekhari [1], Mahmoud Memariani [1,*], Zahra Maleki [1], Mohsen Aleali [1], Pooria Kianoush [2,3], Adel Shirazy [4,5], Aref Shirazi [4] and Amin Beiranvand Pour [6]

[1] Department of Earth Sciences, Science and Research Branch, Islamic Azad University, Tehran 1477893855, Iran; eftekhari.h1395@gmail.com (S.H.E.); zmaleki.iau@gmail.com (Z.M.); aleali.mohsen@gmail.com (M.A.)
[2] Department of Petroleum and Mining Engineering, South Tehran Branch, Islamic Azad University, Tehran 1584743311, Iran; pooria.kianoush@gmail.com
[3] National Iranian Oil Company, Exploration Directorate (NIOC-EXP), Tehran 1994814695, Iran
[4] Department of Mining Engineering, Amirkabir University of Technology (Tehran Polytechnic), Tehran 1591634311, Iran; adel.shirazy@gmail.com (A.S.); aref.shirazi@aut.ac.ir (A.S.)
[5] Geophysical Institute, Karlsruhe Institute of Technology (KIT), 76131 Karlsruhe, Germany
[6] Institute of Oceanography and Environment (INOS), Higher Institution Center of Excellence (HICoE) in Marine Science, University Malaysia Terengganu (UMT), Kuala Nerus 21030, Terengganu, Malaysia; beiranvand.amin80@gmail.com
* Correspondence: mahmoud.memariani@gmail.com; Tel.: +98-9125377215

Abstract: The crucial parameters influencing drilling operations, reservoir production behavior, and well completion are lithology and reservoir rock. This study identified optimal reservoir rocks and facies in 280 core samples from a drilled well in the Asmari reservoir of the Mansouri field in SW Iran to determine the number of hydraulic flow units. Reservoir samples were prepared, and their porosity and permeability were determined by measuring devices. The flow zone index (FZI) was calculated for each sample using MATLAB software; then, a histogram analysis was performed on the logarithmic data of the FZI, and the number of hydraulic flow units was determined based on the obtained normal distributions. Electrical facies were determined based on artificial neural network (ANN) and multi-resolution graph-based clustering (MRGC) approaches. Five electrical facies with dissimilar reservoir conditions and lithological compositions were ultimately specified. Based on described lithofacies, shale and sandstone in zones three and five demonstrated elevated reservoir quality. This study aimed to determine the Asmari reservoir's porous medium's flowing fluid according to the C-mean fuzzy logic method. Furthermore, the third and fourth flow units in the Asmari Formation have the best flow units with high reservoir quality and permeability due to determining the siliceous–clastic facies of the rock units and log data. Outcomes could be corresponded to the flow unit determination in further nearby wellbores without cores.

Keywords: Asmari sandstone reservoir; litho–electrical facies; MRGC and ANN clustering; hydraulic flow units; optimal reservoir rocks; FZI and FCM clustering

Citation: Eftekhari, S.H.; Memariani, M.; Maleki, Z.; Aleali, M.; Kianoush, P.; Shirazy, A.; Shirazi, A.; Pour, A.B. Employing Statistical Algorithms and Clustering Techniques to Assess Lithological Facies for Identifying Optimal Reservoir Rocks: A Case Study of the Mansouri Oilfields, SW Iran. *Minerals* **2024**, *14*, 233. https://doi.org/10.3390/min14030233

Academic Editor: Xiaomin Zhu

Received: 23 January 2024
Revised: 15 February 2024
Accepted: 24 February 2024
Published: 25 February 2024

1. Introduction

The petroleum industry uses the hydraulic flow unit implication to improve permeability prediction for wells with coreless intervals [1]. A hydraulic unit (geometrical shape of the hole) is defined as the main volume of the entire reservoir rock, in which the petrophysical and geological properties affecting the fluid flow are constant and normally varied in different hydraulic units [2–6]. The change in the characteristics of the cavity geometry determines the existence of separate regions (flow units) with fluid flow characteristics. The classical separation of rock formations is based on geological observations and empirical

relationships between permeability and porosity logs [1,7–9]. However, a rock formation determined for each permeability and porosity may show different values, indicating the presence of several flowing units. The concept of fluid flow units is a powerful and unique tool for dividing the reservoir into units that estimate the internal structure of the reservoir at a scale compatible with reservoir simulation modeling [4,10–14]. Geological texture, mineralogy, sedimentary structures, facies, layered contact surface, nature of permeable barriers, and petrophysical properties of porosity, permeability, and capillary pressure often define flow units [2,13–19]. In clustering, the goal is to achieve a criterion for the most suitable classification of variables or samples based on the most significant similarity within the intergroup and the most remarkable difference between the groups. This characteristic helps us classify variables and samples in clusters with the maximum possible similarity within themselves and the maximum difference between them [10,20–26].

Hossain, et al. [27] utilized fuzzy C-mean in subsurface electrofacies lithological classification. Temizel, et al. [28] classified facies as 3D digital reservoir images, employing the classification of different facies with various unsupervised and supervised learning algorithms. Hussain, et al. [21] identified reservoir rocks for lithofacies prediction by machine learning techniques. Zhang, et al. [29] utilized a 2D training image of the multi-point geostatistics (MPG) method to model the facies of a tight sandstone reservoir. Liu, et al. [30] analyzed influencing reservoir electrical parameters in a Quaternary mudstone reservoir containing biogas. Xing, et al. [31] employed machine learning of core and log data for reservoir rock classification. Krivoshchekov, et al. [32] characterized complex carbonate reservoirs employing reservoir rock groups. Mehmood, et al. [33] studied Quaternary sedimentary facies, including the depositional environment and architectural elements. Xie, et al. [34] discovered diagenetic facies in a developed mixed shale reservoir. Vukadin, et al. [35] employed synthetic wellbore machine learning to present a high-porosity sandstone reservoir's lithology distribution model. Wang, et al. [36] investigated the coupled relationships between tectonic fracture characteristics, sand bodies, and sedimentary microfacies in a braided river delta. Kumar, et al. [37] employed fuzzy C-means clustering as an unsupervised machine learning algorithm for a multi-scale geological mapping of potential field data under sediment litho-units [37,38].

In addition, in recent years, other clustering methods such as fractal geometry have been used in petroleum exploration, employing the results of seismic geophysics, exploratory geochemical prospecting, and geomechanical studies [4,8,13,19,26,39]. Some recent work by Kianoush, et al. [4] used velocity–volume (V–V) cube fractal models to assess the seismic inversion velocity data of the South Azadegan field in SW Iran. Furthermore, in 2022–2023, Kianoush, et al. [25] used the results of seismic velocity investigations and geophysical and petrophysical studies to present a pressure–volume (P–V) cube fractal model including pore pressure, fracture pressure, and other formation pressures. Also, Hosseini, et al. [17] utilized hybrid fractal models for geochemical and geophysical prospecting studies in NE Iran.

This research employs the fuzzy C-mean clustering technique to determine reservoir rock groups in the Mansouri field as a case study. Considering that the flow zone index (FZI) and the number of hydraulic flow unit methods depend on the user (this number changes according to the user's opinion and experience), the possibility of making errors in the calculations is high. For this purpose, to reduce the errors, the sum of square errors parameter was employed to define the number of hydraulic flow units. Then, linear regression analysis was performed on the data, and the squared error's sum was calculated. A similar method for the number of other categories was used, and eventually, a graph of the sum of squared errors against the number of categories was drawn. In these graphs, from one value to the next, the changes in the sum of squared errors are not noticeable and can be ignored. This value is the optimal number of hydraulic flow units. Then, considering that one of the most critical parameters in determining reservoir rock is porosity and permeability, the definition of optimal reservoir rock based on these two parameters employs the fuzzy c-mean clustering method in the MATLAB R2021a software environment.

Thus, each cluster produced during the clustering process represents a reservoir rock. In the clustering process of this method, each reservoir rock has characteristics related to the range, standard deviation, median, mean, maximum, and minimum of porosity and permeability changes, which separates it from other groups. In addition, in the cross-plots of porosity versus permeability, each group is well separated from the other groups, and there is no overlap. It is evident that, in this case, any reservoir rock represents a facies with a specific range in terms of porosity and permeability.

2. Geological Setting of the Case Study Area

The Mansouri field in the southernmost part of the north Dezful zone, about 45 km south of Ahwaz, is located approximately on the border of the Arabian Plate, and Quaternary alluviums represent the Zagros Plate and its surface outcrop. The Mansouri field is located north of the Ahwaz field, in the west, in the vicinity of the Abteymur and Susangerd fields, and northeast of the Shadegan field [40–42]. The Asmari carbonate Formation is an Oligocene and Miocene period hydrocarbon reservoir in western Zagros mountain that primarily consists of marly limestone, dolomite, dolomitic limestone, and limestone [25,41,43,44].

Furthermore, there are smaller amounts of limey sandstone, lithic sandstone, and anhydrite. It has been producing oil since the 1930s. It also forms a significant aquifer, discharging at various springs in the Zagros region. The Asmari Formation's basic biostratigraphy was established in the 1950s and was formally described in 1965. It contains carbonate platforms that were formed in six distinct stages [42,45,46].

It is named after the Asmari Mountains SE of Masjed-i-Soleiman (MIS), and its type sample was taken from the Tang-e-Gel Torsh in these mountains [47]. The Asmari Formation was deposited when the Tethys Ocean finally closed. The Zagros Mountains were first rising. The area was a shallow ocean, gradually less profound during this period. This process culminated in the sea shrinking to lagoons by the time of the succeeding Gachsaran Formation [43,48].

In SW Zagros, the Oligo-Miocene Asmari Formation sits atop the Paleocene Pabdeh Formation. In the Luristan and Fars regions, the Asmari Formation sits atop the Jahrum and Shahbazan Formations. The Asmari Formation is thickest in the NE part of the Dezful Embayment [13,23,24,40,43,46]. The location, stratigraphic column, and reservoir zonation of the Mansouri oil field are presented in Figure 1A,B for one of the drilled wells. The Bangestan reservoir was subdivided into nine zones in the studied field based on petrography, petrophysical parameters, and well-logging data.

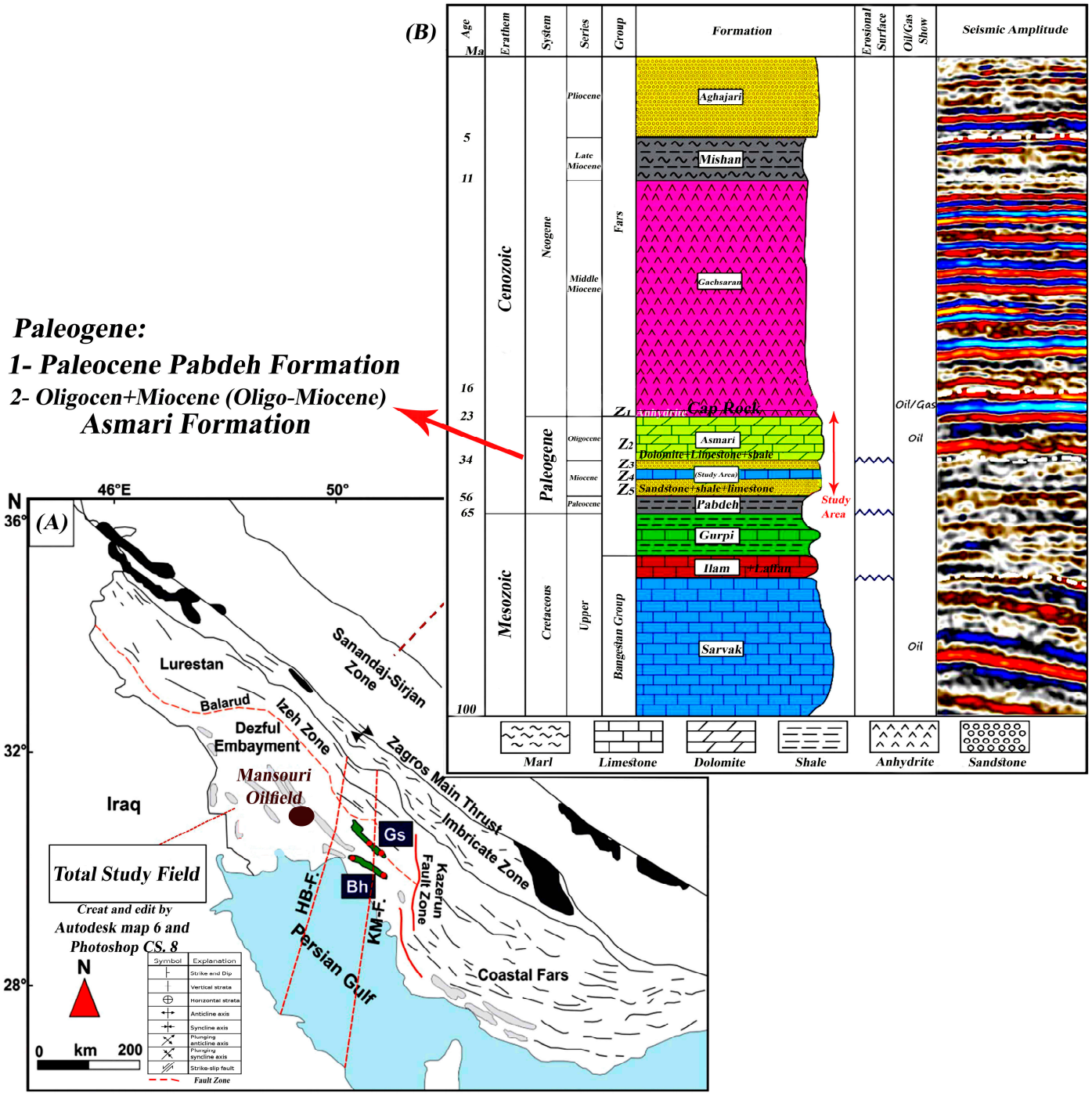

Figure 1. (**A**) The geographical location of the Mansouri oilfield in the Dezful embayment, SW of Iran, and (**B**) a general stratigraphic column of the Mansouri oilfield [23,40,43].

3. Materials and Methods

Determination of facies is one of the main elements of oil exploration and reservoir property determination. Electrical facies or electrofacies are specified employing petrophysical logs such as resistivity, gamma ray, neutron-density, and acoustic logs and can be attributed to one or more lithofacies. Electrofacies and lithofacies are utilized in reservoir characterization, but they have some key differences. Electrofacies use wireline logging technology and artificial intelligence (AI) to categorize reservoir rocks. They are employed to study reservoir zonation and can help identify high-quality reservoir zones. On the other hand, lithofacies refer to the classification of reservoirs based on their physical properties

and depositional environment. This method involves the analysis of core samples and thin sections to characterize the lithology of the rocks. While electrofacies can be derived from well logs, lithofacies require additional detailed analysis and examination of the rocks. Electrofacies can provide a broader understanding of reservoir characteristics, while lithofacies provide more specific information about the composition and distribution of different rocks within the reservoir [7,14,22,40,49]. In this study, 280 core samples (acquired from one of the wells of the Mansouri oilfield) were selected to determine hydraulic flow units. Furthermore, information on permeability, porosity, and structural properties was recorded. The general flowchart of this study is presented in Figure 2.

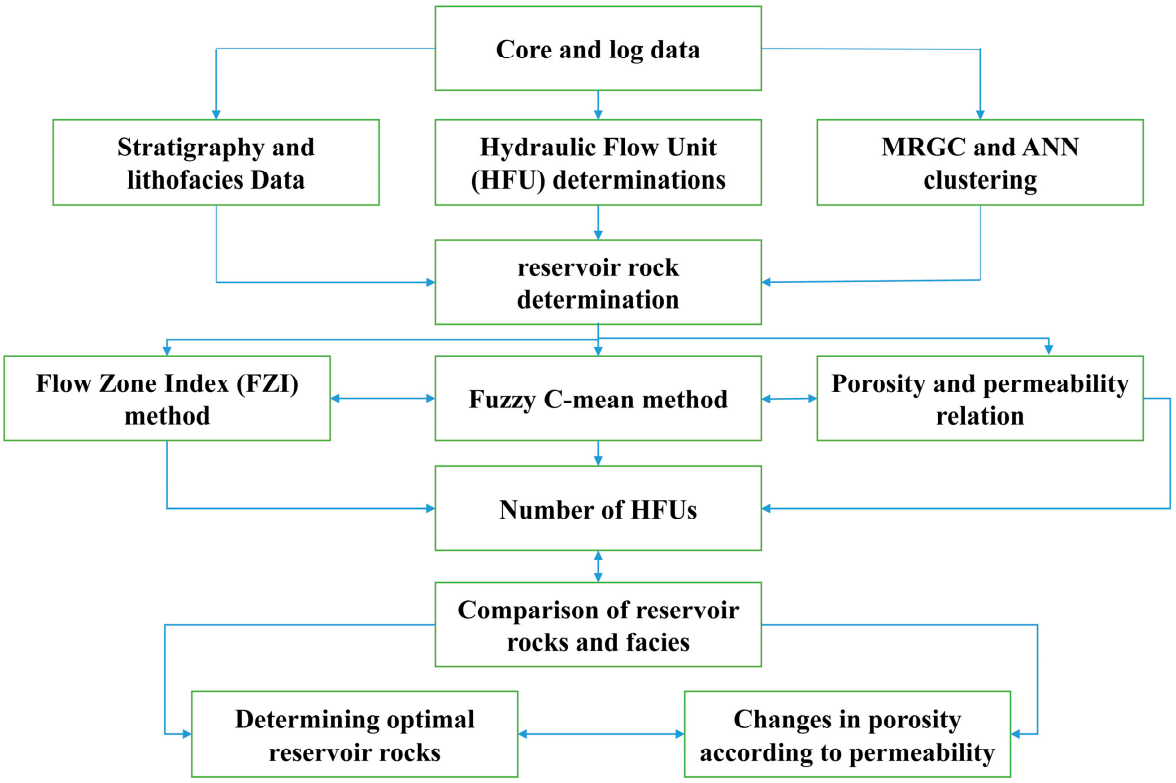

Figure 2. General flowchart of the study according to log and core data in the well.

3.1. Determination of the Number of Hydraulic Flow Units

The methods of determining the number of hydraulic flow units include histogram analysis, normal probability analysis, and sum of squared errors (SSE). All three methods are studied on core data. Based on Figure 3A, a histogram analysis is performed on the logarithmic data of the flow area index. The first hydraulic flow unit includes 24 members, the second hydraulic flow unit includes 109 members, the third hydraulic flow unit includes 117 members, and the fourth hydraulic flow unit includes 30 members. In the normal probability analysis method for assessing the data of the logarithm of the flow area index, four linear distributions are obtained, which indicate four units of hydraulic flow (Figure 3B). According to Figure 3C, in the method of sum of squares of errors calculated according to the number of hydraulic flow units, the value of SSE in the presence of one hydraulic flow unit is equal to 0.92 to check the behavior of insufficient hydraulic flow and by increasing the number of hydraulic flows to four, the lowest value of SSE is 0.002; adding more to the value of HFUs causes insignificant changes in the value of SSE (Table 1).

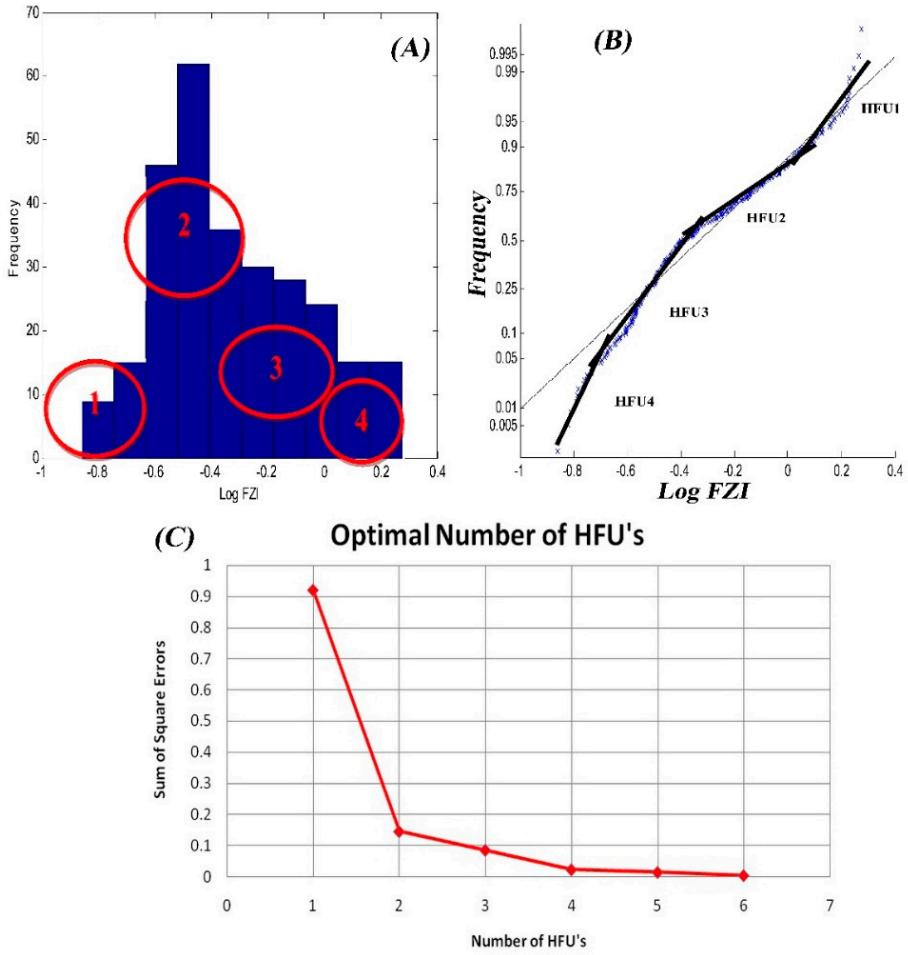

Figure 3. (**A**) Logarithmic data histogram analysis of the flow zone index (four hydraulic flow unit), (**B**) normal probability analysis of the flow zone index. The blue crosses indicate the overall data of the hydraulic flow units, the light gray line indicates the general linear fit of the data, and the four bold black lines indicate the best linear fit for each hydraulic flow unit, and (**C**) optimum hydraulic flow unit no. (HFU) based on the sum of squared errors (SSE).

Table 1. The value of the error calculated for the number of hydraulic flow units.

Hydraulic Flow Unit (HFU) No.	Sum of Squared Errors (SSE)
1	0.92131
2	0.14451
3	0.0846
4	0.02171
5	0.01331
6	0.00299

According to the results obtained from these three methods, the sum of squared errors method is the optimal method for determining the number of hydraulic flow units because it is independent of the user and has higher accuracy in determining the number of categories.

3.2. Determining Optimal Reservoir Rocks (Groups)

After determining the number of hydraulic flow units, we used two methods to determine optimal reservoir rocks, which include:

3.2.1. Flow Zone Index (FZI) Method Per Flow Unit

Ideally, if the values of the reservoir quality index and the porosity ratio are drawn on a log–log scale, the data that have the same values of the flow zone index are placed on a line with a single slope, and samples with different flow zone index values are placed on parallel lines. The samples that are on the same line have the same pore throat properties and therefore make a hydraulic flow unit. Each line defines a unique HFU and the width from the origin of the lines at Φz = 1 shows the average value for that unit [1,3,20].

To obtain an equivalent value of FZI for each group, when we plot RQI in terms of Φz in a logarithmic graph, we must obtain a line with a constant slope of 45 degrees, which is at Φ = 50% (that is, Φ = 1) of the value Log Φz becomes zero, as a result, Log RQI becomes equal to Log FZI. Using this method, the FZI equivalent to each unit of hydraulic flow can be obtained. In order to obtain a line with an angle of 45 degrees, where the scattering of points to draw this line is volumetric, the deviation formula can be used (Equation (1)). Results for each HFU is presented in Table 2 and Figure 4.

$$LogRQI = Log\varphi_z + LogFZI \quad (1)$$

where: Φz is the ratio of pore volume to grain volume, FZI is considered an indicator of the flow zone, and RQI is the Reservoir Quality Index (in micrometers) [8,50–52].

Table 2. FZI values for each hydraulic flow unit.

Hydraulic Flow Unit	Flow Zone Index (FZI)
1	0.1899
2	0.3117
3	0.6345
4	1.4459

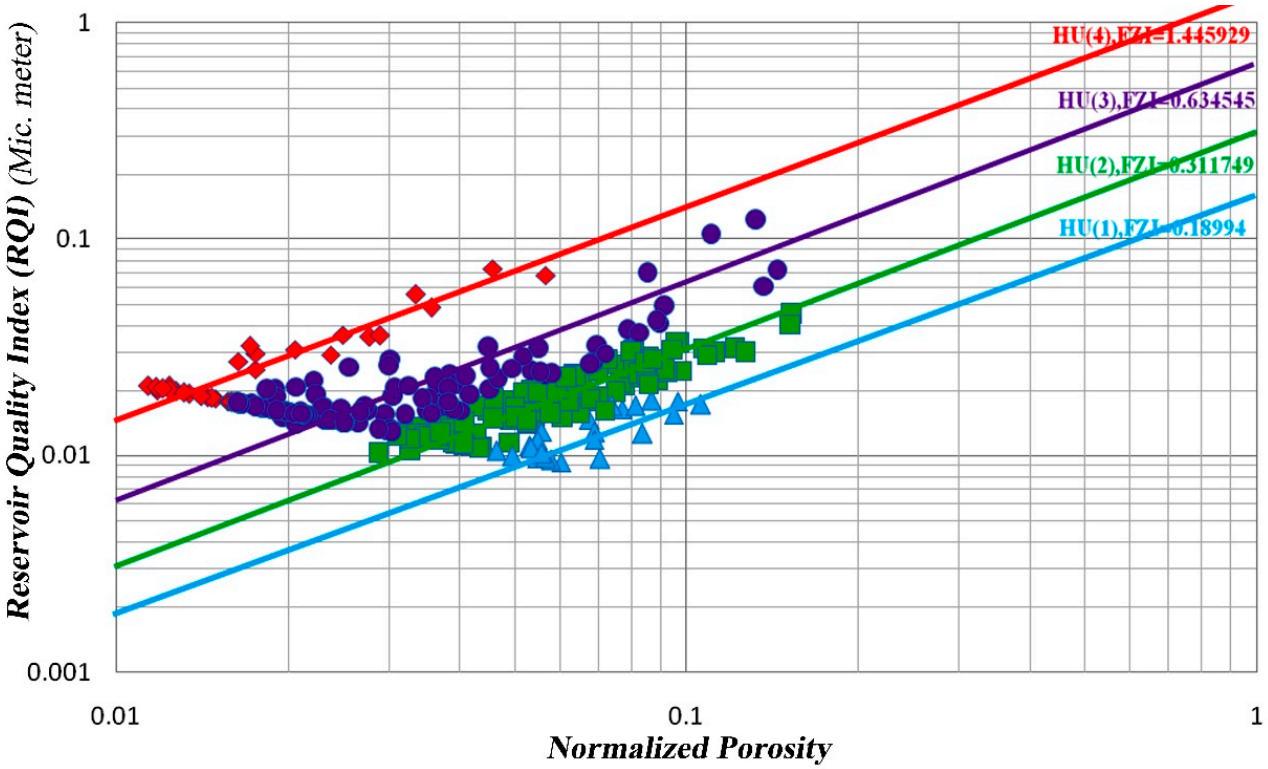

Figure 4. FZI of HFU 1 to HFU 4 in well #A of the Asmari Formation.

By using this method, the FZI equivalent for each unit of hydraulic flow can be obtained. In order to obtain a line with an angle of 45 degrees, where the scattering of points to draw this line is volumetric, the deviation formula can be used (Equation (2)).

$$\sum Err = \sum (Y - y)^2 = S \quad (2)$$

where: E_{rr} is the error (deviation), Y is the actual RQI of each sample, and y is the estimated RQI of each sample [21,51–53]. Classification of samples for HFUs 1 to 4 are presented in Tables S1–S4.

Porosity and permeability data have different dimensions, so they should be normalized between 0 and 1 before correlation; the normalized J-function for porosity data has been used.

3.2.2. Fuzzy C-Mean Method (FCM)

The fuzzy c-mean clustering method is proposed to solve the problem that each data point is assigned to a specific cluster in each iteration. In the FCM clustering algorithm, the number and centers of clusters are determined by the user at first. The quality of this algorithm strongly depends on the initial number of clusters and the initial location of the cluster centers [11,24,37,54]. The objective function describes the distance from any provided data point to a cluster center weighted as the data point's membership grade (Equation (3)):

$$\begin{aligned} &Obj{\cdot}Func = \sum_{i=1}^{c} \sum_{j=1}^{n} u_{ij}^{m} \|x_j - c_i\|^2 \\ &1 \le i \le c \\ &1 \le j \le n \end{aligned} \quad (3)$$

where u_{ij} denotes the membership of pixel x_j in the j_{th} cluster, v_i is the i_{th} cluster center, $\|.\|$ is a norm metric, and m is a constant [24,37]. The parameter m handles the fuzziness of the resulting partition, and m = 2 is utilized in this study (Table 3).

Table 3. Evaluation function (J_m) values for consecutive iterations.

Iteration Count	Obj. Function
1	8.8759
2	6.9395
3	6.6943
4	5.8739
5	4.9493
6	4.3072
7	3.8888
8	3.7368
9	3.6962
10	3.6846
11	3.6806

As seen in Figure 5, the fuzzy c-mean algorithm divides the data set into 4 similar fuzzy clusters, which have different numbers of members. In this diagram, each cluster is displayed with a separate color, and the centers of each cluster are marked with a black square. The first cluster with blue color has 77 members, the second cluster with red color has 42 members, the third cluster with green color has 87 members and the fourth cluster with pink color has 74 members.

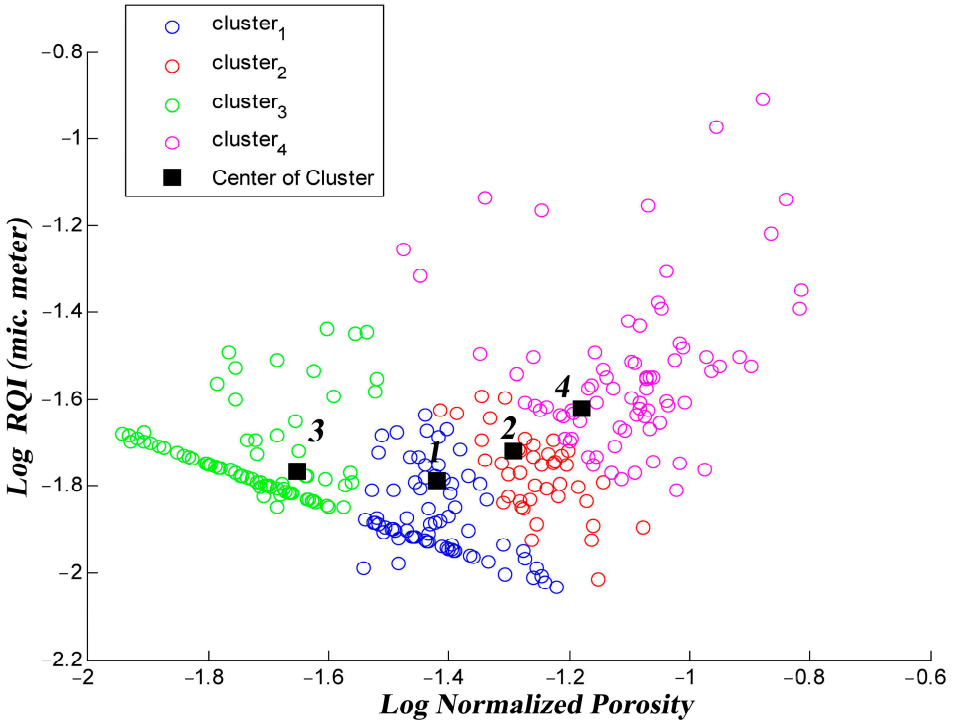

Figure 5. Four identical fuzzy clusters with different members according to the fuzzy c-means method.

3.3. Determining the Lithological and Electrical (Litho–Electrical) Facies Number by Clustering Algorithms

Electrical facies numbers depend on employed well logs and the spatial statistical distribution nature of the data [22,40,55]. Additional clustering algorithms with a trial-and-error process could identify and separate sedimentary facies to study thin sections prepared from core samples (lithofacies). One geological strategy is explaining and preparing the reservoir rock with this restricted information [45,55–57]. Moreover, four depositional sedimentary environments deposited on a platform with a low slope are distinguished based on thin section and lithofacies study in the Asmari Formation of Mansouri oilfield. Furthermore, this study employs an electrical facies model utilizing well logs and two clustering methods in a drilled well with coring to present the optimal reservoir rocks of the studied field.

This research used multi-resolution graph base and artificial neural network (MRGC and ANN) clustering methods to determine electrical facies. The MRGC is one of the few non-parametric and very suitable methods for studying and analyzing data clusters obtained from well logs and drilling cores. This clustering method divided facies with common geological/reservoir conditions into categories by reading gamma, neutron, density, acoustic, and resistivity logs.

Data clustering is the basis of modeling and classification algorithms. In this method, the data of the graphs are determined by two indices: neighborhood index (NI) and Kernel representative index (KRI). NI determines the proximity of each point in a data set to the peak or trough of the possible density function of the data. KRI is an index to choose the data points for representation defined as the core or center of the cluster. KRI is estimated by employing the Equation (4).

$$KRI(x) = NI(x) \cdot M(x,y) \cdot D(x,y) \quad (4)$$

where $M(x, y) = m$, when y is the m_{th} neighbor of x, and $D(x, y)$ is the x and y *distance* [7,22,32,58,59].

Also, in the present study, which was based on the ANN clustering method, assuming eight optimal facies in the previous stage, an estimate for the facies in the entire well was made by building an ANN model between the petrophysical logs and the facies log of the last step. The Levenberg–Marquardt (L–M) algorithm trains the data to construct the neural network model. This network has three layers (input, hidden, and output). The number of neurons was also calculated through trial and error and response optimization. The artificial neuron has a P input and an output [31,49,60].

The inputs are x_i (i = 1, . . ., p), and the output is y_j. The relationship between inputs and outputs can be set as follows (Equation (5)):

$$\begin{cases} S_j = \sum_{i=1}^{p} w_{ij} \cdot x_i - \theta_j \\ y_j = f(S_j) \end{cases} \quad (5)$$

Here θ is the threshold. W_{ij} is the weight of the connection from signal i to neuron j. S_j is pure activation, and f (S_j) is the activation function. The Feed-Forward Back Propagation Artificial Neural Network (FFBPANN) is employed as a famous ANN applicable in petroleum engineering [26,35]. The structure or topology of the employed MRGC and ANN is shown in Figure 6A,B.

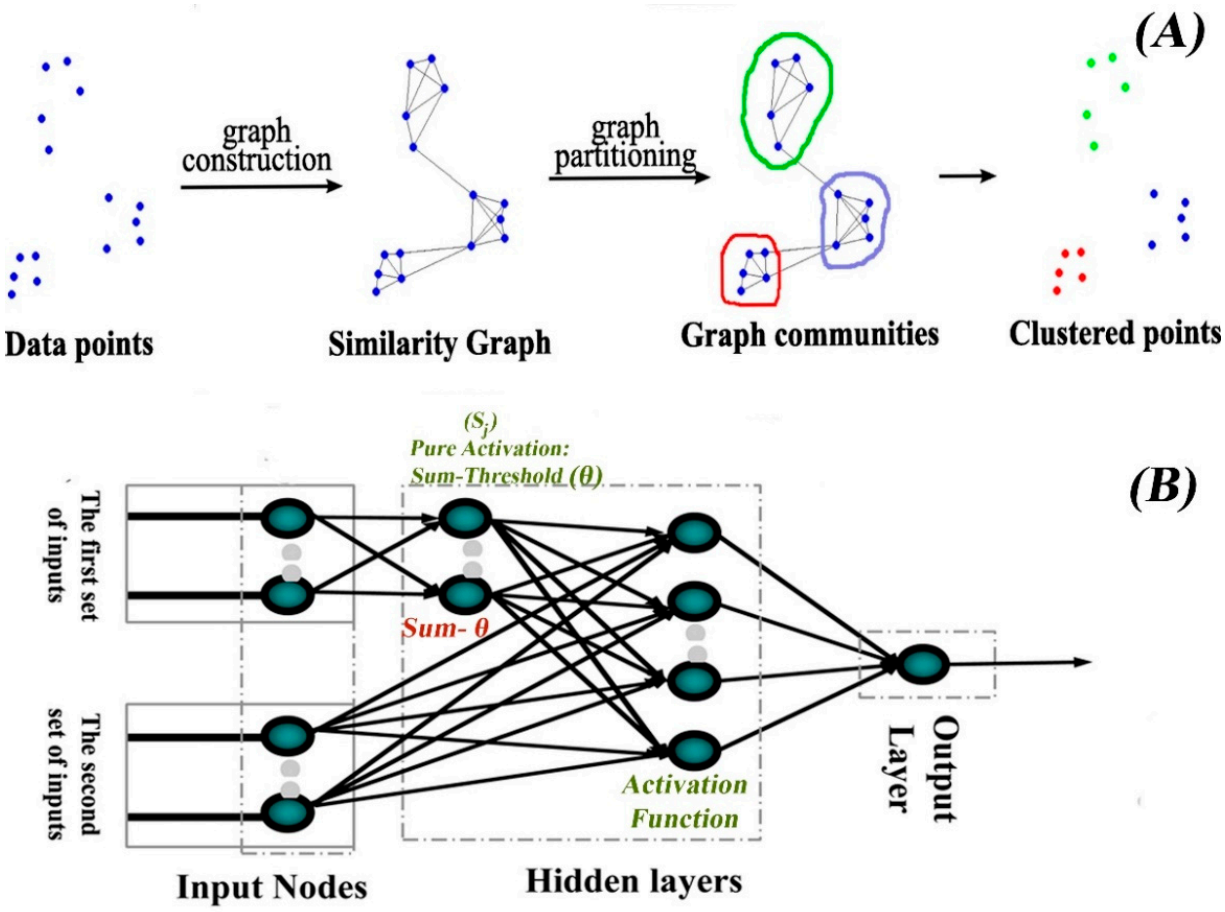

Figure 6. (**A**) Multi-resolution graph-based data clustering (MRGC) via multi-scale community detection, (**B**) FFBP-ANN structure [22,26].

Detailed comparative explanations about the specific advantages and limitations of these two methods are presented in Table 4.

Table 4. Advantages and limitations of MRGC and ANN clustering in determining electrofacies [1,5,22,24,26,27].

MRGC Clustering Advantages	Limitations	ANN Clustering Advantages	Limitations
Capability of identifying natural patterns in the logs with no need for prior knowledge about the data	Time complexity of the algorithm, which can be time-consuming	Can enhance clustering performance by leveraging the representational power of neural networks	Number of clusters to be distinguished by the algorithm must be known
An automatic suggestion of the best number of clusters	One-way irreversibility of the algorithm	Trained network can produce the desired output for new inputs	Highly sensitive to initial conditions and distinctions among data points
Lowest parameters and insensitivity to their changes	Once clusters are merged, they cannot be separated again	An intelligent analysis with simple mathematical methods addressing nonlinear, fuzzy, and complex relationships	Can be computationally and memory intensive
No restrictions on the type or number of data and clusters	Requires the final cluster number, which is often unknown in advance	Can be used in real-time applications	Often limited by the graph constructed on the original features
Allows for results under different resolutions without the need for a predetermined number of clusters	May struggle with handling clusters of varying densities and scalability	Can be used to approximate centralized clustering schemes in distributed decision-making processes	Challenges in scenarios where the graph is unavailable

4. Results

Outcomes of hydraulic flow units were made based on 280 core samples and well logs acquired from one of the exploratory wells in the Mansouri field. Moreover, determining facies is one of the main components of oil exploration and determination of reservoir properties. To overcome the issue of limited data, integrated analysis of FCM and FZI clustering techniques is helpful for developing the porosity correlation to predict the optimal reservoir rocks without core wells. Based on the general results of the determination of reservoir rocks (groups), the total continuity number of the fuzzy c-mean method is higher than the flow zone index at depth and shows more excellent continuity.

4.1. Stratigraphy and Zoning

Employing Geolog software (7.v2011.1, Paradigm, Milan, Italy), the lithology is evaluated and estimated for each stratigraphic column using corrected logs and lithology cross-sections (neutron-density, Rho-U, MID, and MN plots). Finally, employing the probabilistic method, the petrophysical parameters are calculated for the whole sequence, and the average of these parameters is calculated for the whole well and each zone.

According to petrophysical outcomes, the Asmari Formation is divided into five zones with identifying production zones.

Zone 1 exists in all drilled wells and consists of anhydrite, dolomite, and a thick layer of limestone. Zone 2 is also present in all wells, mainly dolomite and sandstone. Zone 3's dominant lithology includes shale, limestone, and sandstone. Zone 4 also exists in all wells, containing sandstone and shale with a barrier/beach ridge, and is likely to be associated with the Ahwaz sand dunes. Eventually, Zone 5's lithology is shale, sandstone, and limestone, which cannot be identified in all wells due to a lack of logging data (Figure 7).

The average calculated petrophysical parameters of the investigated zones in well A are indicated in Table 5 to compare shale volume, porosity, saturation water, and oil volume in all five investigation zones. When evaluating the quality of sandstone reservoirs based on petrophysical data, it is essential to check the connection between the shale volume (V_{sh}), oil volume (U_{oil}), porosity (PHIE), and water saturation (SWE) parameters. In this way, the shale volume, porosity, and oil volume parameters should be increased, and water saturation should be reduced in each zone in a dependent manner. Therefore, with

the preliminary analysis of zones 1 and 2, which simultaneously have water saturation of 91.8–99%, low porosity of 2.4–3.9%, shale volume of 2.7–18.1%, and worse conditions overall, the shallow volumes of oil are 0.001–0.1%, and they are excluded from the studies in terms of reservoir quality.

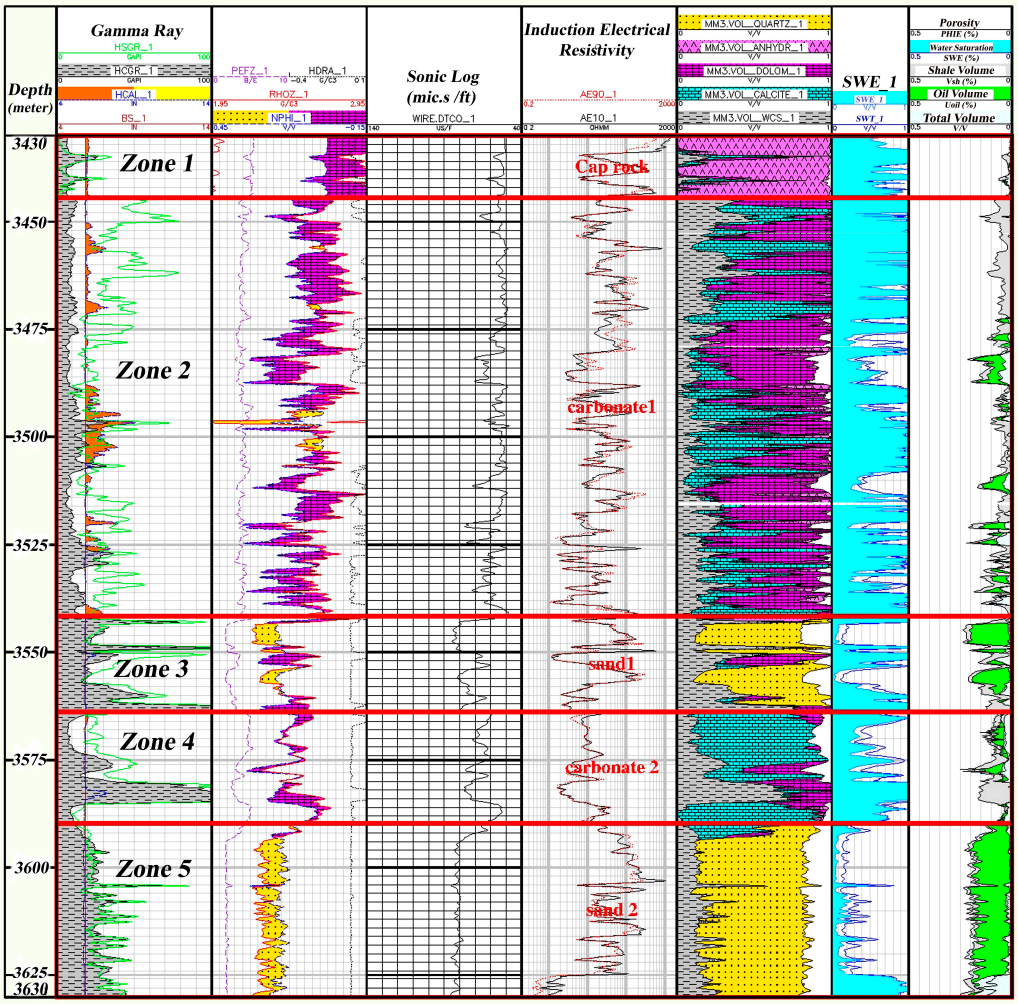

Figure 7. Zoning sequences of the Asmari Formation based on lithological and electrical (litho–electrical) facies in the Mansouri Field.

As represented in Table 5, a maximum in the shale volume (27.4% and 29.4%), porosity (13.1% and 12.9%), oil volume (7.4% and 6.3%), and minimum water saturation (46.5% and 63%) demonstrates the clear distinction between these two zones and other zones in terms of the reservoir capacity of the sandstone and shale in them. The main reservoir zones with dominant shaley sandstone lithology are in zones three and five, respectively.

Table 5. The Asmari Formation's average petrophysical parameters in different zones.

Interval (m)	Zone	Shale Volume Vsh (%)	Porosity PHIE (%)	Water Saturation SWE (%)	Oil Volume Uoil (%)
3427.5–3444.5	1	2.7	2.4	99	0.01
3444.5–3560.5	2	18.1	3.9	91.8	0.055
3560.5–3570.5	3	27.4	13.1	46.5	7.4
3570.5–3585	4	11.5	8.9	76.7	2.9
3585–3630	5	29.5	12.9	63	6.3

4.2. Determining Electrofacies by Clustering Methods

To determine the electrofacies with the MRGC and ANN clustering methods, first in the FACIMAGE™ section of the Geolog software, among the petrophysical logs, those logs that are most related to the results target, which include the gamma ray log (CGR_COR), sonic log (DT.CO), density log (RHO_COR), neutron log (NPHI), and water saturation log (SW_CT), are selected. Facies with common geological/reservoir properties are classified employing the mentioned log readings. Figure 8A,B show the frequency diagrams of the input logs of the model and cross diagrams of these logs, respectively.

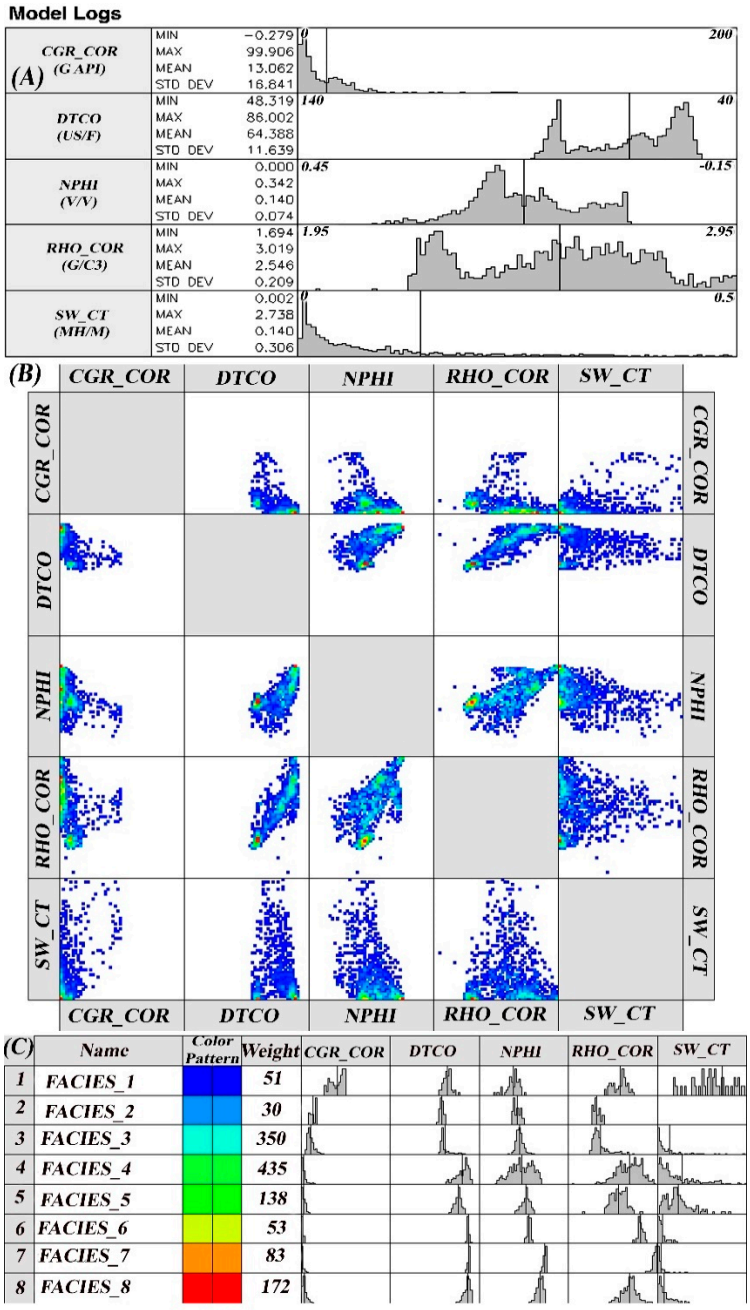

Figure 8. (**A**) Frequency diagram of model input logs, (**B**) cross−over diagram of model input logs relative to each other, (**C**) facies produced by the MRGC method.

Based on the MRGC and ANN clustering methods, the upper and lower limits of the optimal data and models are determined. Finally, applying these models produced two optimal models with eight facies, respectively. An ANN model between petrophysical

logs and pre-facies logs is constructed based on the ANN clustering method. In constructing the neural network model, the Levenberg–Marquardt (L–M) algorithm is used to train the data. This network has three layers (input, hidden, and output). The number of neurons is calculated through trial and error and response optimization as 2-5-1 (Figure 6B). The results of categorized facies are presented in Figure 8C, which shows the readings of each model input log in the separated facies with their weight.

5. Discussion

5.1. MRGC and ANN Clustering Description

Electrofacies are compared to the lithofacies produced by the lithological column and the saturated and hydrocarbon columns. Comparing lithological columns in sandstone and carbonate lithologies and facies columns is clearly illustrated.

Figure 9 shows the correlation and comparison of the zoning results of all three Geolog software calculations, MRGC, and ANN clustering techniques. However, the number of MRGC and ANN electrical facies classifications and lithofacies of the Geolog is different; similar results for the correct separation of anhydrite, limestone, and sandstone are noticed, especially in zones three and five with dominant sandstone lithology.

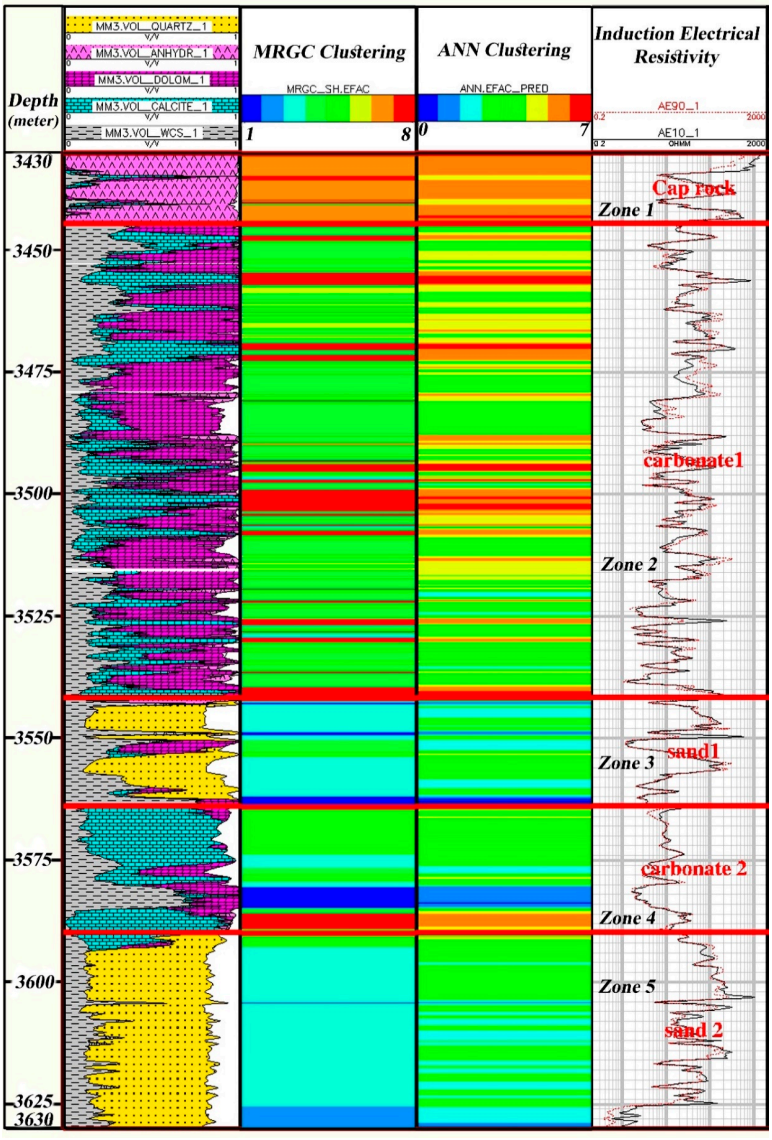

Figure 9. Comparing zoning results of the Geolog software calculations, MRGC, and ANN clustering techniques for the Asmari Formation.

5.2. Comparing Optimal Reservoir Rock Methods

In this research, the integration of two flow zone index (FZI) and fuzzy C-mean (FCM) methods has been utilized to define the proper reservoir rocks in the studied well. HFU lateral continuity of reservoir units with consistent geological properties utilizing the Testerman method is used to control the behavior of fluid flow in pore media laterally. FZI and FCM results showed four hydraulic flow units. Suppose each unit has a maximum continuity number of 1; in that case, their total continuity number becomes 4, and if each of these four units has no continuity between their data, their total continuity becomes zero.

Implementing the FZI data at depth, the continuity numbers for the first to fourth hydraulic flow unit are 0.67, 0.80, 0.77, and 0.53, respectively. Summing up the continuity numbers of these four units, the total continuity number is 2.77 (Table 6). Accordingly, for the FCM technique, the continuity numbers for the first to fourth hydraulic flow units are 0.87, 0.62, 0.90, and 0.73, and the total continuity number is 3.12 (Table 6).

Table 6. Continuity numbers for the hydraulic flow units according to the a) flow zone index (FZI), and fuzzy C-mean (FCM) techniques.

Continuity	Flow Unit 1	Flow Unit 2	Flow Unit 3	Flow Unit 4	Total Cohesion
Flow zone index (FZI)	0.6666	0.7981	0.7692	0.5333	2.7672
Fuzzy C-mean (FCM)	0.8701	0.619	0.8965	0.7297	3.1153

As discussed in the results, the total continuity number of the flow zone index (FZI) method is less than that of the fuzzy c-mean (FCM) technique and demonstrates better continuity at depth. Figure 10 shows the implementation of HFU continuity according to depth.

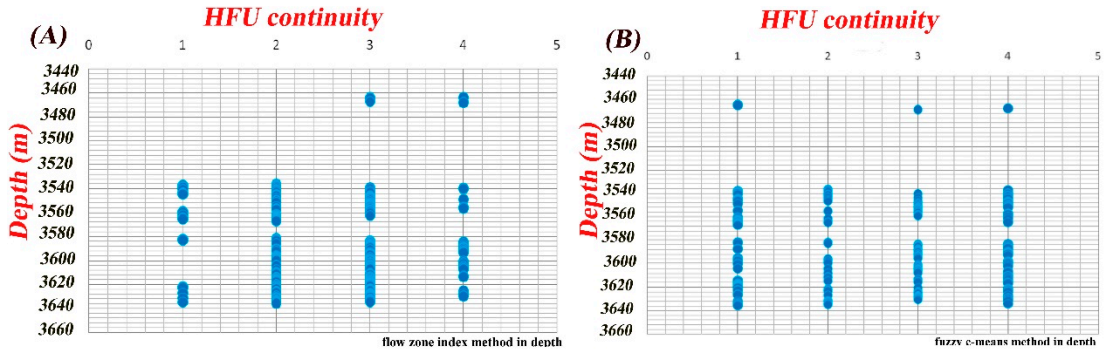

Figure 10. Implementation of (**A**) the FZI method according to depth, (**B**) FCM method according to depth.

As depicted in Figure 10A,B, apart from the upper depths of the Asmari Formation, where it was impossible to drill cores due to mud circulation loss (formation loss), the HFU continuity of units 4 and 1 was lower for the FZI method than for similar cases according to the FCM method. Units 3 and 4 are almost the same in terms of HFU continuity.

5.3. Changes in the Porosity Diagram According to Permeability

Permeability–porosity diagrams in heterogeneous carbonate reservoirs are usually scattered with poor correlation but correlate with the classification and arrangement of data regarding hydraulic flow units [60]. Employing the hydraulic flow unit (HFU) techniques in this research demonstrates better scattering correlations between permeability and porosity diagrams in heterogeneous carbonate reservoirs.

Samples of permeability are observed in hydraulic flow unit Nos. 3 and 4 (Figure 11A–D). Also, Table 7 indicates the correlation coefficients of porosity with permeability for all samples and four HFUs in the studied well.

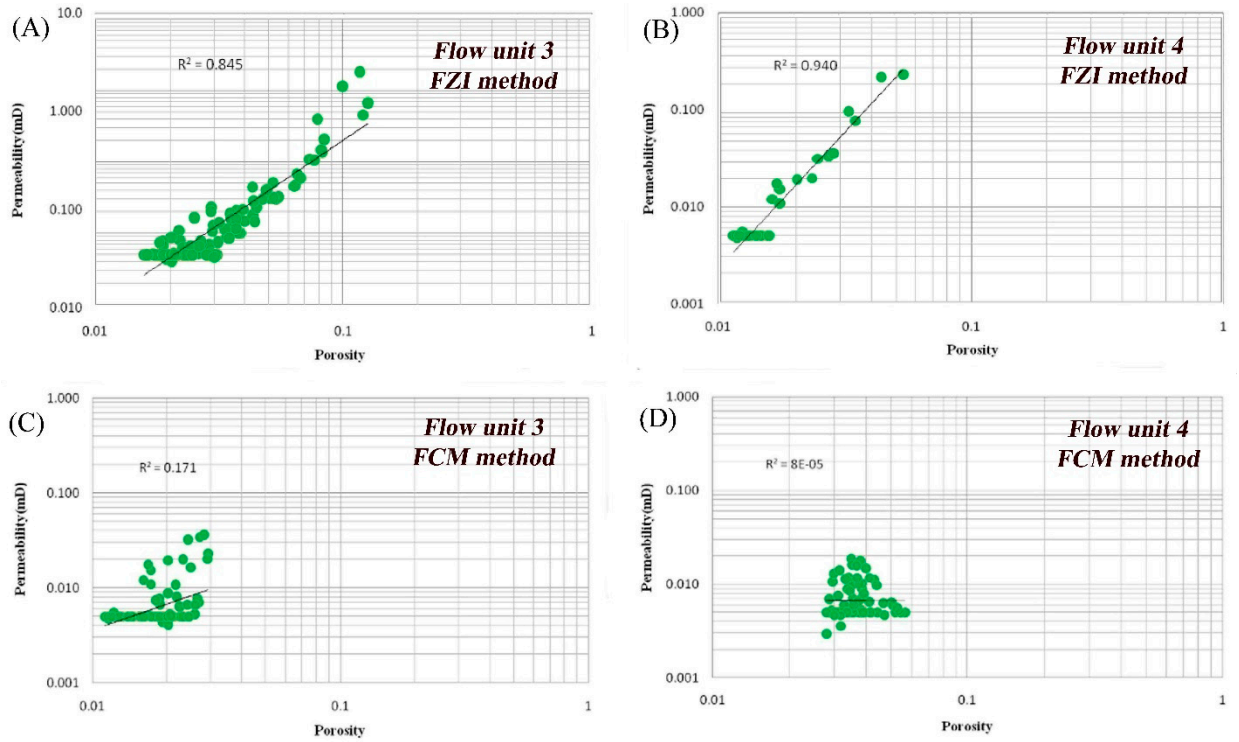

Figure 11. Samples of porosity vs. permeability relationship for each flow unit using the FZI method for (**A**) unit No. 3 and (**B**) unit No. 4 and using the FCM method for (**C**) unit No. 3 and (**D**) unit No. 4.

Table 7. Correlation coefficients of porosity with permeability according to the flow zone index and fuzzy c-mean methods.

Porosity and Permeability Correlation (r)	Flow Unit 1	Flow Unit 2	Flow Unit 3	Flow Unit 4	All Samples
FZI method	0.809	0.939	0.845	0.94	0.552
FCM method	0.195	0.094	0.171	0.00008	

The correlation coefficient for all samples is obtained at 0.552, while with the flow zone index (FZI) method, the first to last HFUs are 0.809, 0.939, 0.845, and 0.94, respectively. It denotes the improvement in the relationship between permeability and porosity in all hydraulic flow units corresponding to the unrestricted state for total samples.

Correspondingly, for the fuzzy c-mean (FCM) method, the first to last HFUs are 0.195, 0.094, 0.171, and 0.00008, respectively. These outcomes indicate that the acquired correlation coefficients of the FCM method in all four HFUs are lower than in the general case.

Based on these results, the flow zone index method improved the correlation coefficients between permeability and porosity in all hydraulic flow units relative to the correlation coefficients in the general states for all samples. However, the fuzzy c-mean method not only did not improve the relationship between the petrophysical parameters of the reservoir in all hydraulic flow units relative to the general states but also reduced the porosity–permeability relationship. Furthermore, according to the results, the total fidelity of the fuzzy c-means method is greater than the total fidelity of the flow zone index at depth and shows greater consistency at depth.

In the FZI clustering results, data with more spatial statistical likenesses are placed into one group, and necessarily, there is no exact relationship between porosity and permeability in each cluster. The hydraulic flow unit with higher FZI values will have a better quality to flow the fluids through its pore spaces in the reservoir rock. The data are well classified, and a satisfactory relationship exists between porosity and permeability for each hydraulic flow unit obtained through FZI curves. As per previous studies, some individual fuzzy models could be developed for each flow unit. A field application confirms that the method can be applied to permeability prediction using well data from various depositional environments. The fuzzy logic technique is instrumental in predicting permeability and identifying permeable and non-permeable zones employing well-log data. As a new strategy for employing core data, an FCM clustering method was helpful in reservoir rock definition in the Asmari Formation for the at-depth HFU continuity. As the correlation between porosity and permeability in this field is not improving, more studies should be conducted to evaluate limitations in the FCM.

Figure 12 shows the optimal reservoir rocks, hydraulic flow unit (HFU), and permeability vs. porosity variations as a petrophysical log in the studied formation in the Mansouri oilfield. At 3560–3444.5 m and 3585–35,705 m intervals (stratigraphy zones 2 and 4), coring was not possible because of the lost circulation, and only the data of the drilling cuttings, and log were used. The dispersion of rock samples in reservoir rock 2 was more than that of others.

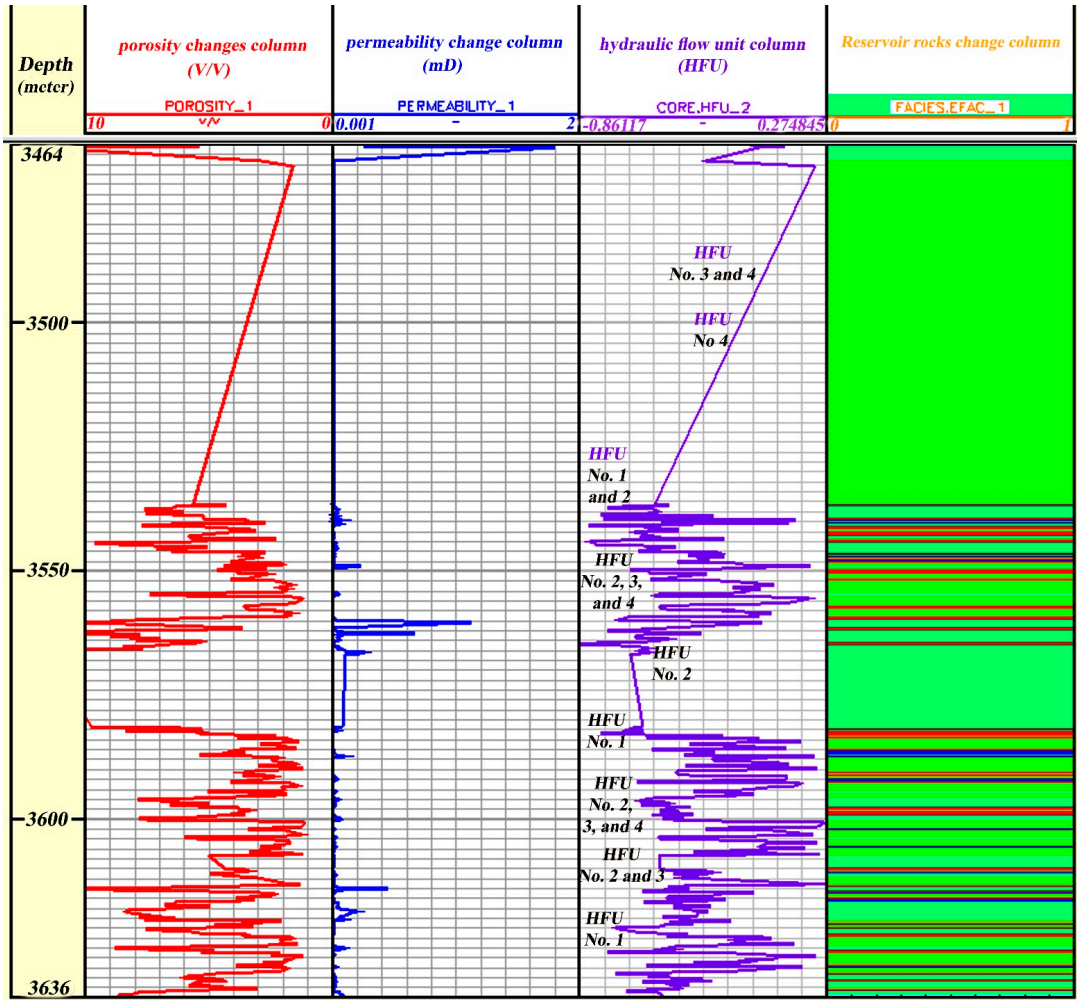

Figure 12. Petrophysical parameter log in exploratory well A, which contains the depth, porosity, permeability, hydraulic flow unit, and reservoir rock change columns (reservoir rock 1: blue, reservoir rock 2: green, reservoir rock 3: navy blue, and reservoir rock 4: red).

5.4. Validating Results Employing Petrographic Analysis Description

This research identifies eleven general petrographic analyses by studying the thin sections of the Asmari Formation in well A. Two general petrofacies and microfacies in this well are siliceous–clastic petrofacies and carbonate–evaporitic, examined by clastic and carbonate components.

The siliceous petrofacies data are employed to validate the results with the presumption that the electrofacies are not necessarily coupled to the lithofacies and that different facies can be placed inside a precise clustering zone. Moreover, another assumption is that the FZIs are not necessarily related to the facies and that different facies can be placed inside a specific flow unit.

Siliceous–clastic petrofacies are described as:

Quartz Arenite: This microfacies includes more than 95% quartz. Quartz particles are frequently angular with proper welding. In this field, sandstones are usually seen as loose sand and sandstones with carbonate or sulfate cement. Due to the texture maturity and appropriate particle melting, these facies can be attributed to a coastal environment with high energy by appropriate particle melting and texture maturity (Figure 13A,B).
Sublitharenite: These facies include carbonate and clastic particles with skeletal grains (Figure 13C).
Siltstone: In the Asmari Formation, this petrofacies is generally deposited in low-energy environments and mainly noticed in the lower parts, and its amount decreases towards the top of the formation (Figure 13D).

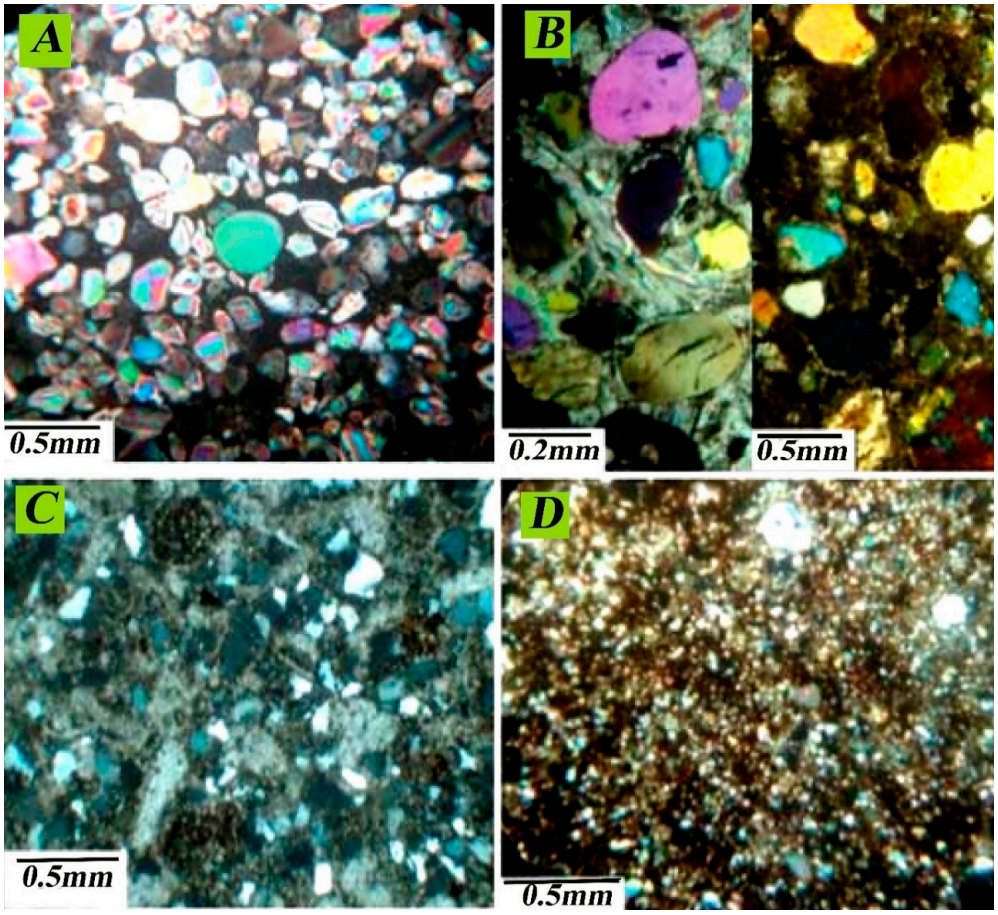

Figure 13. (**A**) Microfacies without cement quartz arenite, (**B**) microfacies of quartz arenite with dolomite cement and sulfate, (**C**) petrofacies of sublitharenite, and (**D**) petrofacies of siltstone in well A, Mansouri oilfield.

As discussed, the porosity and permeability in the determined flow units show a good correlation coefficient. Therefore, in this way, different cavity systems with different petrophysical characteristics can be separated in the studied well, and the facies with the best reservoir conditions can be determined.

The third and fourth HFUs have the best flow units with high reservoir quality and permeability among the appointed flow units. Thus, the depth of the Asmari Formation in the Mansouri oilfield predominantly contains dolomite and sandstone in their facies. The sedimentary environment and its diagenesis process are critical factors affecting them.

Approaches such as cement dolomitization, hydrocarbon migration to the reservoir before sandstone cementation, and dissolution have improved the quality of the reservoir in the Ahwaz sandstone section, which can be noticed in the assessed thin section (Figure 14 A–D). Generally, the determined flow units are influenced by diagenesis processes and the type of porosity created by these processes.

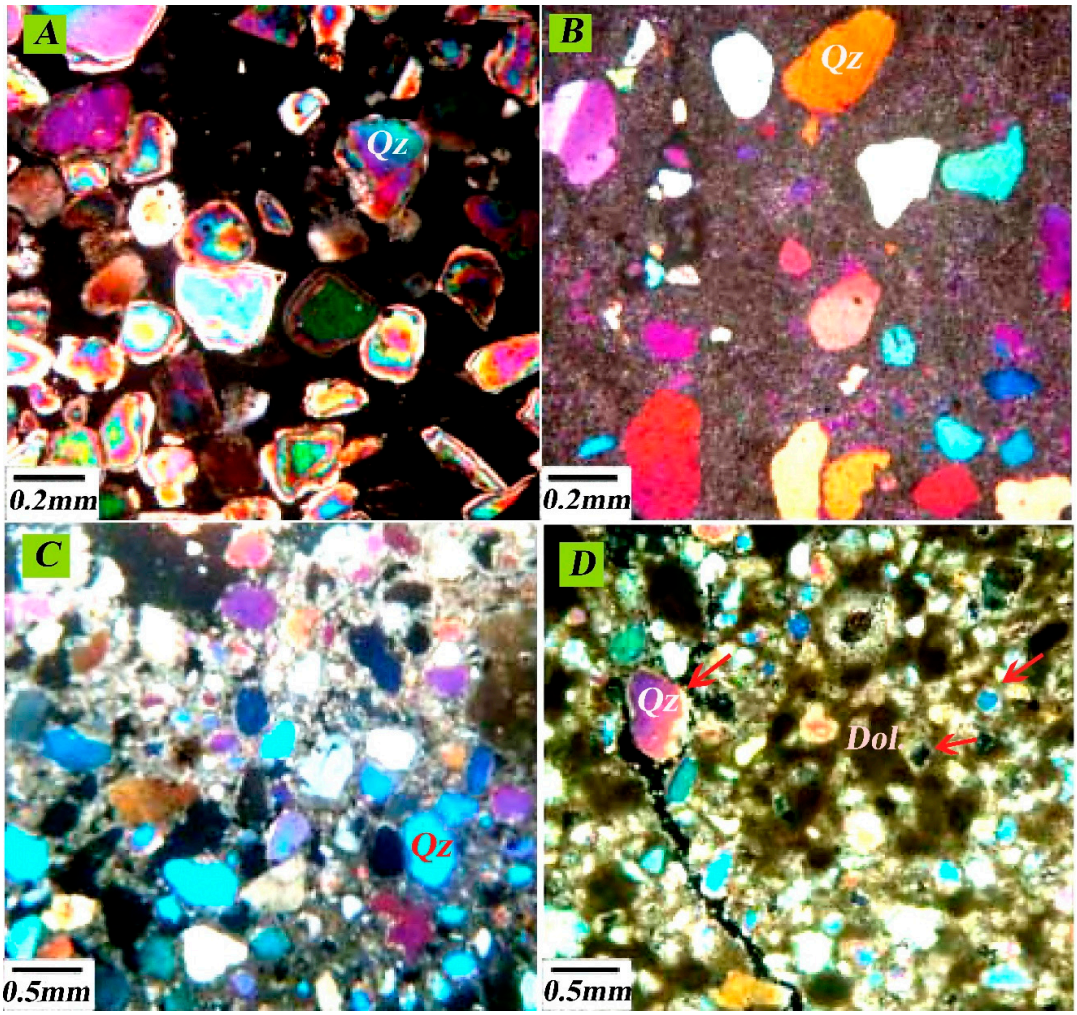

Figure 14. Thin sections of (**A**) without cement sandstones with migrating hydrocarbons before cementing, (**B**) dissolution in sandstones, (**C**) dolomite cement in sandstones, and (**D**) dolomite dissolution in sandstones (The red arrows on the right indicate dolomite (Dol), and the left indicates quartz (Qz)) in the Asmari Formation of the Mansouri oilfield.

6. Conclusions

Litho–electrical facies are valuable approaches for recognizing and determining intervals with comparable petrophysical log responses and roughly equivalent lithologies within a formation almost homogeneous in composition and empty of bio-stratigraphic indicators or marker beds. Consequently, the confined lithofacies are influenced by dia-

genesis approaches and the process of porosity type. Based on a petrophysical study of 280 core samples from one of the exploratory wellbores drilled in the Asmari reservoir located in the Mansouri field, the following results are summarized:

- Four hydraulic flow units were determined for the studied data after classifying the flow zone index amount by the normal probability analysis, histogram analysis, and the sum of squares errors (SSE) procedures.
- Flow zone index (FZI) and fuzzy c-means (FCM) techniques were used to determine optimal reservoir rocks in the study well. Although the FCM method delivers more consistency with depth than the FZI method, the FZI technique enhances the correlation coefficients (r) of porosity relation with permeability in each hydraulic flow unit (HFU).
- The potential zones with high oil accumulation are identified by employing shear limits of shale volume, effective porosity, and water saturation in the Asmari Formation.
- Hydraulic flow units (HFUs) 3 and 4, determined by the FZI method, are more compatible with dolomite and sandstone facies due to the migration time of hydrocarbons being before cementation.
- The MRGC method is more accurate and successful than ANN in determining measured and estimated parameters in the wellbores. Furthermore, it is not limited to data size, numbers, or high operation speed.
- Comparing lithofacies and ANN and MRGC electrofacies demonstrates comparable outcomes of proper separation of anhydrite, limestone, and sandstone, particularly in zones three and five with prevailing sandstone lithology.
- Siliceous lithofacies are utilized to validate data, assuming that the electrofacies are not necessarily coupled to the lithofacies and that different facies can be positioned inside a distinct clustering zone. Consequently, most of the facies at the depths of zones 3 and 5, including sandstone and dolomite facies, demonstrate similar results with electrofacies clustering.

It is recommended that core and log data from nearby wells in the Asmari Formation be employed to assess and inspect the precision of reservoir rock determination more accurately utilizing FZI and FCM. Likewise, it is achievable to employ MRGC and ANN clustering zones to determine sandstone reservoirs in nearby drilled wells and generalize the results to coreless wells in the Asmari Formation of the Mansouri oilfield. Correspondingly, sonic, density, and neutron logs reveal sound reservoir quality at depths where the superb flow units extend. Accordingly, it is possible to utilize hydraulic flow units to define reservoir rocks in cored wells and generalize the outcomes to coreless wells.

Furthermore, as another suggestion, the results obtained from FCM and FZI methods can be compared with clustering methods such as K-means and hierarchy. Additionally, considering the positive results of velocity–volume and pressure–volume fractal methods in recent years, the presentation of electrofacies–volume and hydraulic flow unit–volume fractal approaches can also be evaluated in future studies.

Moreover, regarding potential impacts on petroleum exploration and reservoir management, discussing the practical applicability and feasibility of the results for future similar works is recommended.

Supplementary Materials: The following supporting information can be downloaded at: https://www.mdpi.com/article/10.3390/min14030233/s1, Table S1. Classification of samples in HFU 1; Table S2. Classification of samples in HFU 2; Table S3. Classification of samples in HFU 3; Table S4. Classification of samples in HFU 4.

Author Contributions: All authors have contributed to writing and editing this article. S.H.E.—conceptualization, programming, analysis, writing, and editing; M.M.—supervision, analysis; Z.M.—review and editing; M.A.—supervision, editing; P.K., A.S. (Adel Shirazy), A.S. (Aref Shirazi), and A.B.P.—review, editing, and writing. All authors have read and agreed to the published version of the manuscript.

Funding: This research received no external funding.

Data Availability Statement: The following datasets generated and/or analyzed during the current study are available in the Mahmoud Memariani repository as the corresponding author on reasonable request.

Acknowledgments: We acknowledge the Department of Mining Engineering at Amirkabir University of Technology (Tehran Polytechnic) and the Department of Petroleum and Mining Engineering, South Tehran Brach, Islamic Azad University. The authors consider it necessary to express their sincere gratitude to the esteemed experts of the Research Institute Petroleum Industry (RIPI) and Exploration Directorates of the National Iranian Oil Company (NIOC-EXP) for constructive comments to improve the article's scientific level.

Conflicts of Interest: Pooria Kianoush has affiliated with Islamic Azad University (IAU), and National Iranian Oil Company (NIOC-EXP). The authors declare that they have no known competing financial interests or personal relationships that could have appeared to influence the work reported in this paper.

References

1. Amaefule, J.O.; Altunbay, M.; Tiab, D.; Kersey, D.G.; Keelan, D.K. Enhanced Reservoir Description: Using Core and Log Data to Identify Hydraulic (Flow) Units and Predict Permeability in Uncored Intervals/Wells. In Proceedings of the SPE Annual Technical Conference and Exhibition, Houston, TX, USA, 3–6 October 1993. [CrossRef]
2. Kadkhodaie, A.; Kadkhodaie, R. A Review of Reservoir Rock Typing Methods in Carbonate Reservoirs: Relation between Geological, Seismic, and Reservoir Rock Types. *Iran. J. Oil Gas Sci. Technol.* **2018**, *7*, 13–35. [CrossRef]
3. Karimian Torghabeh, A.; Qajar, J.; Dehghan Abnavi, A. Characterization of a heterogeneous carbonate reservoir by integrating electrofacies and hydraulic flow units: A case study of Kangan gas field, Zagros basin. *J. Pet. Explor. Prod. Technol.* **2023**, *13*, 645–660. [CrossRef]
4. Kianoush, P.; Mohammadi, G.; Hosseini, S.A.; Keshavarz Faraj Khah, N.; Afzal, P. Compressional and Shear Interval Velocity Modeling to Determine Formation Pressures in an Oilfield of SW Iran. *J. Min. Environ.* **2022**, *13*, 851–873. [CrossRef]
5. Houshmand, N.; GoodFellow, S.; Esmaeili, K.; Ordóñez Calderón, J.C. Rock type classification based on petrophysical, geochemical, and core imaging data using machine and deep learning techniques. *Appl. Comput. Geosci.* **2022**, *16*, 100104. [CrossRef]
6. Maldar, R.; Ranjbar-Karami, R.; Behdad, A.; Bagherzadeh, S. Reservoir rock typing and electrofacies characterization by integrating petrophysical properties and core data in the Bangestan reservoir of the Gachsaran oilfield, the Zagros basin, Iran. *J. Pet. Sci. Eng.* **2022**, *210*, 110080. [CrossRef]
7. Davis, J.C. Electrofacies in Reservoir Characterization. In *Handbook of Mathematical Geosciences: Fifty Years of IAMG*; Daya Sagar, B.S., Cheng, Q., Agterberg, F., Eds.; Springer International Publishing: Berlin/Heidelberg, Germany, 2018; pp. 211–223. [CrossRef]
8. Pirhadi, A.; Kianoush, P.; Ebrahimabadi, A.; Shirinabadi, R. Wellbore Stability in a Depleted Reservoir by Finite Element Analysis of Coupled thermo-poro-elastic Units in an Oilfield, SW Iran. *Results Earth Sci.* **2023**, *1*, 100005. [CrossRef]
9. Yokeley, B.A.; Ghanbarian, B.; Sahimi, M. Rock Typing Based on Wetting-Phase Relative Permeability Data and Critical Pore Sizes. *SPE J.* **2021**, *26*, 3893–3907. [CrossRef]
10. Jafarzadeh, N.; Kadkhodaie, A.; Ahmad, B.J.; Kadkhodaie, R.; Karimi, M. Identification of electrical and petrophysical rock types based on core and well logs: Utilizing the results to delineate prolific zones in deep water sandy packages from the Shah Deniz gas field in the south Caspian Sea basin. *J. Nat. Gas Sci. Eng.* **2019**, *69*, 102923. [CrossRef]
11. Ji, L.; Lin, M.; Jiang, W.; Cao, G.; Xu, Z.; Hao, F. An improved rock typing method for tight sandstone based on new rock typing indexes and the weighted fuzzy kNN algorithm. *J. Pet. Sci. Eng.* **2022**, *210*, 109956. [CrossRef]
12. Kiaei, H.; Sharghi, Y.; Ilkhchi, A.K.; Naderi, M. 3D modeling of reservoir electrofacies using integration clustering and geostatistic method in central field of Persian Gulf. *J. Pet. Sci. Eng.* **2015**, *135*, 152–160. [CrossRef]
13. Kianoush, P.; Mohammadi, G.; Hosseini, S.A.; Khah, N.K.F.; Afzal, P. Inversion of seismic data to modeling the Interval Velocity in an Oilfield of SW Iran. *Results Geophys. Sci.* **2023**, *13*, 100051. [CrossRef]
14. Madani, N.; Biranvand, B.; Naderi, A.; Keshavarz Faraj Khah, N. Lithofacies uncertainty modeling in a siliciclastic reservoir setting by incorporating geological contacts and seismic information. *J. Pet. Explor. Prod. Technol.* **2019**, *9*, 1–16. [CrossRef]
15. Konaté, A.A.; Ma, H.; Pan, H.; Khan, N. Analysis of situ elemental concentration log data for lithology and mineralogy exploration— A case study. *Results Geophys. Sci.* **2021**, *8*, 100030. [CrossRef]
16. Ahmad, W.; Gingras, M.K. Integrating sedimentology and ichnology with rock typing and flow units: Implications for clastic reservoir characterization. *J. Pet. Sci. Eng.* **2022**, *208*, 109628. [CrossRef]
17. Hosseini, S.A.; Khah, N.K.F.; Kianoush, P.; Afzal, P.; Ebrahimabadi, A.; Shirinabadi, R. Integration of fractal modeling and correspondence analysis reconnaissance for geochemically high-potential promising areas, NE Iran. *Results Geochem.* **2023**, *11*, 100026. [CrossRef]
18. Ojo, B.T.; Olowokere, M.T.; Oladapo, M.I. Sensitivity analysis of changing Reservoir Saturation involving Petrophysics and Rock Physics in 'Royal G' field, Niger Delta. *Results Geophys. Sci.* **2021**, *7*, 100018. [CrossRef]

19. Kianoush, P.; Mohammadi, G.; Hosseini, S.A.; Keshavarz Faraj Khah, N.; Afzal, P. Determining the drilling mud window by integration of geostatistics, intelligent, and conditional programming models in an oilfield of SW Iran. *J. Pet. Explor. Prod. Technol.* **2023**, *13*, 1391–1418. [CrossRef]
20. Amraei, H.; Falahat, R. Improved ST-FZI method for permeability estimation to include the impact of porosity type and lithology. *J. Pet. Explor. Prod.* **2021**, *11*, 109–115. [CrossRef]
21. Hussain, M.; Liu, S.; Ashraf, U.; Ali, M.; Hussain, W.; Ali, N.; Anees, A. Application of Machine Learning for Lithofacies Prediction and Cluster Analysis Approach to Identify Rock Type. *Energies* **2022**, *15*, 4501. [CrossRef]
22. Mahadasu, P.; Singh, K.H. Electrofacies Estimation of Carbonate Reservoir in the Scotian Offshore Basin, Canada Using the Multi-resolution Graph-Based Clustering (MRGC) to Develop the Rock Property Models. *Arab. J. Sci. Eng.* **2022**, *48*, 7855–7866. [CrossRef]
23. Mohammadian, E.; Kheirollahi, M.; Liu, B.; Ostadhassan, M.; Sabet, M. A case study of petrophysical rock typing and permeability prediction using machine learning in a heterogenous carbonate reservoir in Iran. *Sci. Rep.* **2022**, *12*, 4505. [CrossRef] [PubMed]
24. Salavati, Z.; Asadi Mehmandosti, E.; Moallemi, S.A. Determination of rock types using hydraulic flow unit, multi-resolution graph-based clustering, and fuzzy c-mean clustering methods of the Sarvak Formation in an oilfield of Dezful Embayment. *Adv. Appl. Geol.* **2023**, *12*, 925–944. [CrossRef]
25. Kianoush, P.; Mohammadi, G.; Hosseini, S.A.; Keshavarz Faraj Khah, N.; Afzal, P. Application of Pressure-Volume (P-V) Fractal Models in Modeling Formation Pressure and Drilling Fluid Determination in an Oilfield of SW Iran. *J. Pet. Sci. Technol.* **2022**, *12*, 2–20. [CrossRef]
26. Kianoush, P.; Mohammadi, G.; Hosseini, S.A.; Keshavarz Faraj Khah, N.; Afzal, P. ANN-based estimation of pore pressure of hydrocarbon reservoirs—A case study. *Arab. J. Geosci.* **2023**, *16*, 302. [CrossRef]
27. Hossain, T.M.; Watada, J.; Aziz, I.A.; Hermana, M. Machine Learning in Electrofacies Classification and Subsurface Lithology Interpretation: A Rough Set Theory Approach. *Appl. Sci.* **2020**, *10*, 5940. [CrossRef]
28. Temizel, C.; Odi, U.; Balaji, K.; Aydin, H.; Santos, J.E. Classifying Facies in 3D Digital Rock Images Using Supervised and Unsupervised Approaches. *Energies* **2022**, *15*, 7660. [CrossRef]
29. Zhang, N.; Li, S.; Chang, L.; Wang, C.; Li, J.; Liang, B. Study on Facies Modeling of Tight Sandstone Reservoir Using Multi-Point Geostatistics Method Based on 2D Training Image—Case Study of Longdong Area, Ordos Basin, China. *Minerals* **2022**, *12*, 1335. [CrossRef]
30. Liu, J.; Chai, X.; Yang, H.; Gu, D.; Wang, L. Measurement of Rock Electrical Parameters and Analysis of Influencing Factors of Quaternary Mudstone Biogas Reservoirs in Qaidam Basin. *Energies* **2022**, *15*, 9100. [CrossRef]
31. Xing, Y.; Yang, H.; Yu, W. An Approach for the Classification of Rock Types Using Machine Learning of Core and Log Data. *Sustainability* **2023**, *15*, 8868. [CrossRef]
32. Krivoshchekov, S.; Kochnev, A.; Kozyrev, N.; Botalov, A.; Kochneva, O.; Ozhgibesov, E. Rock Typing Approaches for Effective Complex Carbonate Reservoir Characterization. *Energies* **2023**, *16*, 6559. [CrossRef]
33. Mehmood, M.; Naseem, A.A.; Saleem, M.; Rehman, J.u.; Kontakiotis, G.; Janjuhah, H.T.; Khan, E.U.; Antonarakou, A.; Khan, I.; Rehman, A.U.; et al. Sedimentary Facies, Architectural Elements, and Depositional Environments of the Maastrichtian Pab Formation in the Rakhi Gorge, Eastern Sulaiman Ranges, Pakistan. *J. Mar. Sci. Eng.* **2023**, *11*, 726. [CrossRef]
34. Xie, M.; Yang, W.; Zhao, M.; Li, Y.; Deng, Y.; Gao, Y.; Xu, C.; Hou, H.; Yao, L.; Zhang, Z.; et al. Diagenetic Facies Controls on Differential Reservoir-Forming Patterns of Mixed Shale Oil Sequences in the Saline Lacustrine Basin. *Minerals* **2023**, *13*, 143. [CrossRef]
35. Vukadin, D.; Čogelja, Z.; Vidaček, R.; Brkić, V. Lithology and Porosity Distribution of High-Porosity Sandstone Reservoir in North Adriatic Using Machine Learning Synthetic Well Catalogue. *Appl. Sci.* **2023**, *13*, 7671. [CrossRef]
36. Wang, Z.; Lin, X.; Zhu, S.; Fan, J.; Zheng, Y. Coupling Relationships between Sedimentary Microfacies, Sand Bodies, and Tectonic Fracture Characteristics in Braided River Deltas: A Case Study of the Bashijiqike Formation in the Keshen 2 Area. *Minerals* **2023**, *13*, 1020. [CrossRef]
37. Kumar, S.; Arasada, R.C.; Rao, G.S. Multi-Scale Potential Field Data Integration Using Fuzzy C-Means Clustering for Automated Geological Mapping of North Singhbhum Mobile Belt, Eastern Indian Craton. *Minerals* **2023**, *13*, 1014. [CrossRef]
38. Zahaf, K.; Tiab, D. Vertical Permeability From In Situ Horizontal Measurements in Shaly-Sand Reservoirs. *J. Can. Pet. Technol.* **2002**, *41*, 8. [CrossRef]
39. Kianoush, P.; Mahvi, M.R.; Keshavarz Faraj Khah, N.; Kadkhodaie, A.; Jodeiri Shokri, B.; Varkouhi, S. Hydrogeological studies of the Sepidan basin to supply required water from exploiting water wells of the Chadormalu mine utilizing reverse osmosis (RO) method. *Results Earth Sci.* **2024**, *2*, 100012. [CrossRef]
40. Khazaie, E.; Noorian, Y.; Moussavi-Harami, R.; Mahboubi, A.; Kadkhodaie, A.; Omidpour, A. Electrofacies modeling as a powerful tool for evaluation of heterogeneities in carbonate reservoirs: A case from the Oligo-Miocene Asmari Formation (Dezful Embayment, southwest of Iran). *J. Afr. Earth Sci.* **2022**, *195*, 104676. [CrossRef]
41. Laursen, G.V.; Monibi, S.; Allan, T.L.; Pickard, N.A.H.; Hosseiney, A.; Vincent, B.; Hamon, Y.; van Buchem, F.S.P.; Moallemi, A.; Druillion, G. The Asmari Formation Revisited: Changed Stratigraphic Allocation and New Biozonation. *Eur. Assoc. Geosci. Eng.* **2009**, cp-125-00069. [CrossRef]

42. Sadeghi, R.; Moussavi-Harami, R.; kadkhodaie, A.; Mahboubi, A.; Ashtari, A. Reservoir rock typing of the Asmari Formation using integrating geological and petrophysical data for unraveling the reservoir heterogeneity: A case study from the Ramshir oilfield, southwest Iran. *Carbonates Evaporites* **2021**, *36*, 60. [CrossRef]
43. Noorian, Y.; Moussavi-Harami, R.; Hollis, C.; Reijmer, J.J.G.; Mahboubi, A.; Omidpour, A. Control of climate, sea-level fluctuations and tectonics on the pervasive dolomitization and porosity evolution of the Oligo-Miocene Asmari Formation (Dezful Embayment, SW Iran). *Sediment. Geol.* **2022**, *427*, 106048. [CrossRef]
44. Abyat, Y.; Abyat, A.; Abyat, A. Microfacies and depositional environment of Asmari formation in the Zeloi oil field, Zagros basin, south-west Iran. *Carbonates Evaporites* **2019**, *34*, 1583–1593. [CrossRef]
45. Esfandyari, M.; Mohseni, H.; Heidari, M. Facies analysis, depositional sequences and platform evolution of the Sarvak Formation (late Albian-Turonian) in the Zagros Basin, West of Iran. *J. Afr. Earth Sci.* **2023**, *198*, 104811. [CrossRef]
46. Khalili, A.; Vaziri-Moghaddam, H.; Arian, M.; Seyrafian, A. Carbonate platform evolution of the Asmari Formation in the east of Dezful Embayment, Zagros Basin, SW Iran. *J. Afr. Earth Sci.* **2021**, *181*, 104229. [CrossRef]
47. Safari, H.O.; Pirasteh, S.; Pradhan, B.; Gharibvand, L.K. Use of Remote Sensing Data and GIS Tools for Seismic Hazard Assessment for Shallow Oilfields and its Impact on the Settlements at Masjed-i-Soleiman Area, Zagros Mountains, Iran. *Remote Sens.* **2010**, *2*, 1364–1377. [CrossRef]
48. Karimi, H.; Raeisi, E.; Bakalowicz, M. Characterising the main karst aquifers of the Alvand basin, northwest of Zagros, Iran, by a hydrogeochemical approach. *Hydrogeol. J.* **2005**, *13*, 787–799. [CrossRef]
49. Kolbikova, E.; Gusev, S.; Malinovskaya, O.; Garaev, A.; Valiev, R. Lithofacies analysis of Devonian carbonate deposits based on geological and geophysical information analysis by using machine learning methods. *Eur. Assoc. Geosci. Eng.* **2021**, *2021*, 1–6. [CrossRef]
50. Al-Jawad, S.N.; Saleh, A.H.; Al-Dabaj, A.A.A.; Al-Rawi, Y.T. Reservoir flow unit identification of the Mishrif formation in North Rumaila Field. *Arab. J. Geosci.* **2014**, *7*, 2711–2728. [CrossRef]
51. El-Sayed, A.M.A.; Sayed, N.A.E.; Ali, H.A.; Kassab, M.A.; Abdel-Wahab, S.M.; Gomaa, M.M. Rock typing based on hydraulic and electric flow units for reservoir characterization of Nubia Sandstone, southwest Sinai, Egypt. *J. Pet. Explor. Prod. Technol.* **2021**, *11*, 3225–3237. [CrossRef]
52. Esmaeili, B.; Rahimpour-Bonab, H.; Kadkhodaie, A.; Ahmadi, A.; Hosseinzadeh, S. Developing a saturation-height function for reservoir rock types and comparing the results with the well log-derived water saturation, a case study from the Fahliyan formation, Dorood oilfield, Southwest of Iran. *J. Pet. Sci. Eng.* **2022**, *212*, 110268. [CrossRef]
53. Hussain, S.; Muhammad Khan, N.; Emad, M.Z.; Naji, A.M.; Cao, K.; Gao, Q.; Ur Rehman, Z.; Raza, S.; Cui, R.; Salman, M.; et al. An Appropriate Model for the Prediction of Rock Mass Deformation Modulus among Various Artificial Intelligence Models. *Sustainability* **2022**, *14*, 15225. [CrossRef]
54. Kadkhodaie, A.; Rezaee, R.; Moallemi, S.A. A fuzzy logic approach for estimation of permeability and rock type from conventional well log data: An example from the Kangan reservoir in the Iran Offshore Gas Field. *J. Geophys. Eng.* **2006**, *3*, 356–369. [CrossRef]
55. Al-Iessa, I.A.; Zhang, W.Z. Facies evaluation and sedimentary environments of the Yamama Formation in the Ratawi oil field, South Iraq. *Sci. Rep.* **2023**, *13*, 5305. [CrossRef] [PubMed]
56. Saleh, A.H.; Hemimey, W.A.E.; Leila, M. Integrated Geological and Petrophysical Approaches for Characterizing the Pre-Cenomanian Nubian Sandstone Reservoirs in Ramadan Oil Field, Central Gulf of Suez, Egypt. *Arab. J. Sci. Eng.* **2023**, *48*, 7939–7958. [CrossRef]
57. Opuwari, M.; Afolayan, B.; Mohammed, S.; Amaechi, P.O.; Bareja, Y.; Chatterjee, T. Petrophysical core-based zonation of OW oilfield in the Bredasdorp Basin South Africa. *Sci. Rep.* **2022**, *12*, 510. [CrossRef]
58. Bhattacharya, S.; Carr, T.R.; Pal, M. Comparison of supervised and unsupervised approaches for mudstone lithofacies classification: Case studies from the Bakken and Mahantango-Marcellus Shale, USA. *J. Nat. Gas Sci. Eng.* **2016**, *33*, 1119–1133. [CrossRef]
59. Okhovvat, H.R.; Riahi, M.A.; Akbari Dehkharghani, A. Kernel principal component analysis (KPCA) in electrical facies classification. *Iran. J. Oil Gas Sci. Technol.* **2023**, *12*, 1–17. [CrossRef]
60. Yasmaniar, G.; Sitaresmi, R.; Prakoso, S. Determination of Rock Type Using Hydraulic Flow Unit Concept to Predict Permeability with Artificial Neural Network. *J. Earth Energy Sci. Eng. Technol.* **2018**, *1*, 622–666. [CrossRef]